2003

Electric-field-induced heating and energy relaxation in GaN

T. A. Eckhause
University of Michigan - Ann Arbor

Ö. Süzer
University of Michigan - Ann Arbor

Ç. Kurdak
University of Michigan - Ann Arbor

F. Yun
Virginia Commonwealth University

Hadis Morkoç
Virginia Commonwealth University, hmorkoc@vcu.edu

Eckhause, T.A., Süzer, Ö., Kurdak, Ç., et al. Electric-field-induced heating and energy relaxation in GaN. Applied Physics Letters, 82, 3035 (2003).

Electric-field-induced heating and energy relaxation in GaN

T. A. Eckhause,[a] Ö. Süzer, and Ç. Kurdak
Physics Department, University of Michigan, Ann Arbor, Michigan 48109

F. Yun and H. Morkoç
Electrical Engineering Department, Virginia Commonwealth University, Richmond, Virginia 23284

(Received 11 November 2002; accepted 7 March 2003)

Electric-field-induced heating is studied using noise measurements in *n*-type GaN grown on sapphire substrates. The measured electron temperature is found to be an order of magnitude higher than what is expected based on calculations of electron–phonon coupling via acoustic deformation potential scattering processes in GaN. The discrepancy may be explained by a large thermal boundary resistance between the GaN film and the sapphire substrate. © *2003 American Institute of Physics.* [DOI: 10.1063/1.1571982]

The use of GaN and GaN-based heterostructures in high-power applications has a considerable, if recent, history.[1,2] The study of energy flow between hot electrons and their surroundings is therefore of particular interest in the GaN system. As electrons gain energy through the application of an electric field, they cease to be in equilibrium with the phonons, but equilibrate with each other via electron–electron interactions. This forms a hot electron system whose temperature may significantly exceed that of the lattice phonons.[3,4] The emission of acoustic and optical phonons by a hot electron gas sets the energy relaxation time, which in turn determines the characteristic time for hot electrons to relax to the lattice temperature. At low temperatures, we expect the dominant method of cooling to be the emission of acoustic phonons through acoustic deformation potential scattering. At higher temperatures (above 100 K), we expect the faster emission of polar optical phonons to dominate electron cooling. Energy then flows from the GaN lattice phonons to the phonons in the sapphire substrate before flowing to the bath. Knowledge of the energy relaxation time is of fundamental importance and is also relevant to device design. In high-power devices in particular, understanding the processes that govern the cooling of hot carriers is useful in accessing device performance. Measurements of luminescence,[5] measurements of white noise,[6] Shubnikov-de Haas measurements,[7] and blackbody radiation measurements[8] are commonly used in the GaAs/AlGaAs heterostructure system to determine the temperature of an electron gas in excess of the lattice temperature. Such measurements have not previously been performed for the nitride system.

In this work, we have used the Johnson noise (up to 100 kHz) in a patterned GaN film as an intrinsic thermometer of the *electron* temperature, while the substrate was held in a 4.2-K liquid helium bath. In addition to the study of excess high-frequency noise, we have examined the low frequency, or $1/f$ noise, and compared its value between samples with different electron densities.

All the GaN samples we have studied were grown by molecular-beam epitaxy on sapphire substrates using rf-generated active nitrogen. We present results for three samples: A1, A2, and B. Samples A1 and A2 are patterned from a high-electron-density GaN film grown on *c*-plane sapphire substrate, with a 40-nm AlN buffer layer. The 1.1-μm-thick film is intentionally doped with Si. Sample B, also grown on *c*-plane sapphire, has a more elaborate buffer layer structure consisting of 40-nm AlN, 200-nm GaN, followed by a multiple layer GaN/AlGaN composite. Finally a 0.8-μm GaN layer grown at 800 °C contains the electron gas.

Hall bar patterns with dimensions of 25 μm$\times$250 μm for samples A1 and B, and 50 μm$\times$500 μm for sample A2, were defined by photolithography. Reactive ion etching with BCl_3 etched the exposed region down to the substrate. The original thicknesses of the GaN layers of samples A and B are 1.11 and 1.17 μm, respectively, but after processing their thicknesses were reduced to 0.68 and 0.60 μm, respectively. Metallization of the Ti/Al/Ti/Au contacts was followed by rapid thermal annealing at 90 °C to form good ohmic contact to the GaN. Low-temperature (4.2 K) Hall measurements of the samples revealed electron densities of 4.75×10^{18} and 4.0×10^{17} cm^{-3} for samples A and B, respectively. The results are summarized in Table I.

The diagram of our noise measurement is shown in Fig. 1. The large ($\approx$150 μF) capacitor after the bias stage acts as a short circuit to all ac signals, including the voltage noise of bias resistors. In addition to those elements shown, there are parasitic line capacitances that we have not included in our diagram. The preamplifier used in this setup was made using low-noise junction field-effect transistors (Toshiba 2SK162) in its input stages and had a voltage noise of $4nV/\sqrt{Hz}$. The

TABLE I. The electron density, the mobility, the resistance per square, the GaN film thickness, and the number of electrons in the GaN Hall bar, are listed for the three samples. The density and mobility are measured at 4.2 K using Hall measurements.

Sample	Density (cm^{-3})	μ (cm^2/V s)	$R_\square(\Omega)$	Thickness (μm)	N
A1	4.75×10^{18}	89.0	217	0.68	2.02×10^{10}
A2	4.75×10^{18}	89.0	217	0.68	8.08×10^{10}
B	4.0×10^{17}	143	1817	0.60	1.5×10^{9}

[a]Electronic mail: eckhause@umich.edu

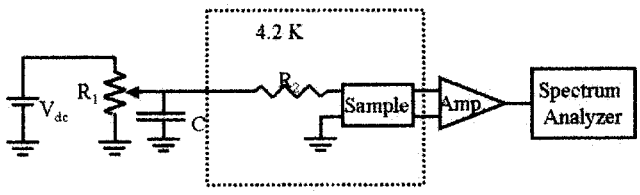

FIG. 1. Block diagram of the noise measurement circuit. R_1 is 5 kΩ; V_{dc} is 32 V; C is 150 μF and R_2 was set to obtain a useful range of bias currents. The samples are four-probe Hall bars.

sample noise amplified by the preamplifier was fed into a Stanford Research 830 spectrum analyzer for Fourier analysis. Each noise spectrum was obtained by averaging 32 000 traces.

The voltage noise spectrum of a sample will generally include both the low-frequency $1/f$ noise and the frequency-independent Johnson noise, proportional to the electron temperature and the sample resistance. The $1/f$ noise in the nitride system has been studied recently by various groups.[9–13] In most of the samples for which we have measured the excess noise, the difference between the noise spectrum at a finite dc bias and the spectrum at zero bias, was dominated by the $1/f$ noise for frequencies less than 100 kHz. Only in a sample with high carrier density was the $1/f$ noise sufficiently small that we were able to observe white-noise components of the excess noise arising from electron heating. Sample B is a representative of several low-electron-density samples, all of which showed large excess low-frequency noise. Typical excess noise spectra obtained from different samples are shown in Figs. 2 and 3.

The magnitude of $1/f$ noise is in general quantified by a dimensionless Hooge parameter, $\alpha = \Delta S_V f N / V^2$, where ΔS_V is the excess noise spectral power density, V is the bias voltage, f is the frequency, and N is the number of electrons in the GaN Hall bar, as listed in Table I. We calculate $\alpha = 1.5 \times 10^{-2}$, 1.2×10^{-4}, and 1.6×10^{-3} for samples B, A2, and A1, respectively. The trend that we observe of α, decreasing with increasing density of electrons, is consistent with other studies of $1/f$ noise in GaN.[13,14]

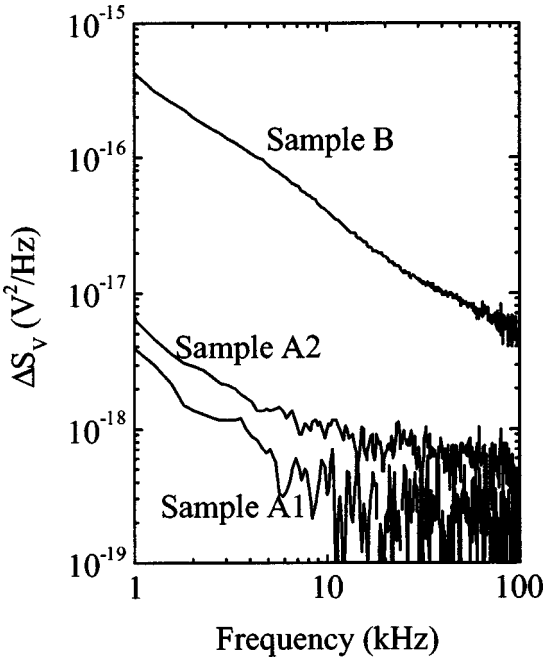

FIG. 2. The excess voltage noise spectra of three samples. The bias currents are 9, 440, and 89 μA for samples B, A2, and A1, respectively. The noise spectra scale approximately as $1/f$ for sample B and for samples A1 and A2 below ~10 kHz. Excess Johnson noise is dominant above ~30 kHz in samples A1 and A2.

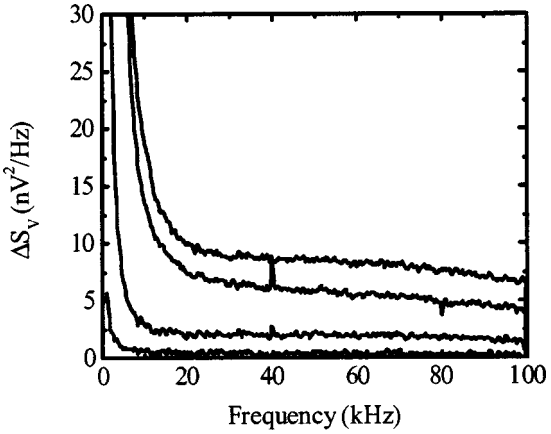

FIG. 3. Measured excess noise at 4.2 K in sample A1 at dc bias currents of 0.13, 0.49, 0.97, and 1.33 mA. Increasing excess noise corresponds to increasing bias current. The bias resistor, R_2 in Fig. 1, is 22 kΩ. Above frequencies of 30 kHz, white noise dominates the low-frequency noise.

In high-electron-density samples A1 and A2, the excess $1/f$ noise was sufficiently small such that the excess frequency-independent Johnson noise could be observed. From the excess noise of samples A1 and A2, we have extracted an excess electron temperature, $\Delta T = \Delta S_V / 4 k_B R$, using the excess noise data above ~30 kHz, where $1/f$ noise is small in these samples. The resistance of the samples are independent of bias over the range of voltages that we apply. In Fig. 4, we plot the excess electron temperature versus the Joule power dissipated per electron for sample A1, the smaller Hall bar, and sample A2, the larger Hall bar. To verify that the measured increase in Johnson noise is due to an increase in electron temperature, we scale the power dissipated in the Hall bar to the number of electrons in each Hall bar (as in Fig. 4). We observed that the excess temperature is independent of the number of electron, as we expect.

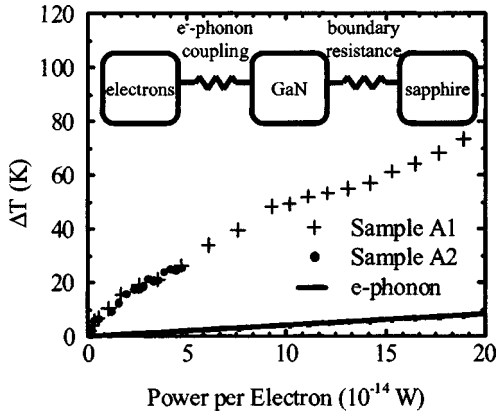

FIG. 4. The excess temperature, $\Delta T = T_{e,\mathrm{GaN}} - 4.2$ K, as a function of power dissipated per electron in samples A1 and A2. The solid line is the calculated temperature difference between the GaN electron and the GaN phonons. The inset shows a schematic diagram of the heat flow from the electrons at $T_{e,\mathrm{GaN}}$ to the phonons at $T_{\mathrm{ph,GaN}}$ to the sapphire substrate at $T_{\mathrm{ph,sapphire}} \approx 4.2$ K.

We compare our data with the expected heat flow from electrons to the lattice via deformation potential electron–phonon coupling. The average power per electron dissipated to the GaN phonons is

$$(P_{\mathrm{disc}})_e = \frac{3m^*\varepsilon_{\mathrm{def}}^2}{2\pi^2\hbar\rho}\left(\frac{2m^*}{\hbar^2}\right)^{3/2}\sqrt{E_{\mathrm{F}}}k_{\mathrm{B}}(T_{e,\mathrm{GaN}} - T_{\mathrm{ph,GaN}}),$$

where $\varepsilon_{\mathrm{def}}$ is the deformation potential constant, ρ is the density, E_{F} the Fermi energy, $T_{e,\mathrm{GaN}}$ is the GaN electron temperature, and $T_{\mathrm{ph,GaN}}$ is the GaN phonon temperature.[15] For GaN, we use $\varepsilon_{\mathrm{def}} = 8.54$ eV and $\rho = 6.1$ g/cm^3, and in our samples we calculate the Fermi energy from the density listed in Table I and an effective mass of $0.22m_0$. We calculate in our samples A1 and A2 that the power, in Watts, dissipated per electron is $(P_{\mathrm{diss}})_e = 2.5\times10^{-14}(T_{e,\mathrm{GaN}} - T_{\mathrm{ph,GaN}})$. If this electron–phonon coupling were limiting the heat flow, we would expect data to fall on the solid line in Fig. 4. Instead, the heating of the electron gas is strikingly larger than is predicted by energy relaxation based on acoustic deformation potential scattering of the hot electrons. The discrepancy can arise from a poor thermal coupling between GaN and sapphire. If the thermal boundary resistance for the GaN–sapphire interface is large, we cannot assume $T_{\mathrm{ph,GaN}} \approx 4.2$ K. To estimate the thermal boundary resistance for this interface, we use a simple model, where $T_{e,\mathrm{GaN}} > T_{\mathrm{ph,GaN}} > T_{\mathrm{ph,sapphire}} = 4.2$ K, shown in the inset of Fig. 4. We first extract $T_{\mathrm{ph,GaN}}$ using the measured $T_{e,\mathrm{GaN}}$ and the theoretical calculation for power dissipation via phonon emission. Then, assuming $T_{\mathrm{ph,sapphire}} \approx 4.2$ K, we extract a thermal boundary resistance of $R_B = 1.05$ K/(W/cm^2) for this interface.

When an interface is smooth and without voids, acoustic mismatch theory provides an estimate of the value of the boundary resistance between dissimilar materials at low temperatures.[16] Such a theory gives a thermal resistance of 3.3×10^{-3} K/(W/cm^2) at 4.2 K between GaN and sapphire. This value is much smaller than indicated by the data. It has been observed in other metal–sapphire interfaces that measured thermal resistances can greatly exceed prediction of acoustic mismatch at temperatures above ~10 K. This discrepancy is attributed to highly disordered interfaces that can strongly scatter phonons.[16] Bulk GaN thermal conductivity has been predicted to depend strongly on the number of dislocations at densities above 10^{12} cm^{-2} at room temperature.[17] At lower temperatures as well, the large lattice mismatch between sapphire and GaN introduces a high degree of interface disorder in the GaN and may contribute to the large thermal boundary resistance evidenced by our data.

We have observed two effects in GaN electron gases grown on sapphire substrates. First, excess low-frequency noise in the bulk of the electron gas varies strongly from sample to sample. Second, we have observed excess noise due to electron heating in high-electron-density samples, where $1/f$ is smaller. The observed large electric-field-induced heating of electrons in GaN indicates that the energy flow is not limited by the acoustic deformation potential electron–phonon scattering. The large heating may instead be due to an additional thermal boundary resistance between the sapphire substrate and the GaN film. This would imply that limiting GaN disorder near the interface may be important in high-power applications, in which increasing heat flow from GaN to a thermal bath is crucial to device performance.

We would like to thank M. Msall for fruitful discussions. The work at the University of Michigan was supported by the Alfred P. Sloan Foundation and by the AFOSR under Contract No. F49620-00-1-0328 through the MURI program. The work at VCU was supported by grants from AFOSR, NSF, and ONR.

[1] S. Nakamura, T. Mukai, and M. Senoh, Appl. Phys. Lett. **64**, 1687 (1994).
[2] W. Kim, O. Aktas, A. Salvador, A. Botchkarev, B. Sverdlov, S. N. Mohammad, and H. Morkoç, Solid-State Electron. **41**, 169 (1997).
[3] M. L. Roukes in *Noise in Physical Systems*, edited by C. M. Van Vliet (World Scientific, Singapore, 1987), pp. 595–604.
[4] P. J. Price, J. Appl. Phys. **53**, 6863 (1982).
[5] J. Shah, A. Pinczuk, H. L. Strömer, A. C. Gossard, and W. Wiegmann, Appl. Phys. Lett. **44**, 322 (1984).
[6] C. Kurdak, D. Tsui, S. Parihar, S. Lyon, and M. Shayegan, Appl. Phys. Lett. **67**, 386 (1995).
[7] H. Sakaki, K. Hirakawa, J. Yoshino, S. P. Svensson, Y. Sekiguchi, T. Hotta, S. Nishii, and N. Miura, Surf. Sci. **142**, 306 (1984).
[8] K. Hirakawa, M. Grayson, D. C. Tsui, and C. Kurdak, Phys. Rev. B **47**, 16651 (1993).
[9] S. L. Rumyantsev, N. Pala, M. S. Shur, R. Gaska, M. E. Levinshtein, M. Asif Khan, G. Simin, X. Hu, and J. Yang, J. Appl. Phys. **90**, 310 (2001).
[10] C. F. Zhu, W. K. Fong, B. H. Leung, C. C. Cheng, and C. Surya, Mater. Res. Soc. Symp. Proc. **622**, T6.23.1 (2000).
[11] B.-H. Leung, W.-K. Fong, C.-F. Ahu, and C. Surya, IEEE Trans. Electron Devices **48**, 2400 (2001).
[12] S. A. Vitusevich, S. V. Danylyuk, N. Klein, M. V. Petrychuk, V. N. Sokolov, V. A. Kochelap, A. E. Belyaev, V. Tilak, J. Smart, A. Vertiatchikh, and F. Eastman, Appl. Phys. Lett. **80**, 2126 (2002).
[13] S. L. Rumyantsev, N. Pala, M. S. Shur, R. Gaska, M. E. Levinshtein, P. A. Ivanov, M. Asif Khan, G. Simin, X. Hu, and J. Yang, Semicond. Sci. Technol. **17**, 476 (2002).
[14] A. P. Dmitriev, E. Borovitskaya, M. E. Levinshtein, S. L. Rumyantsev, and M. S. Shur, J. Appl. Phys. **90**, 301 (2001).
[15] K. Seeger, *Semiconductor Physics: An Introduction* (Springer, New York, 1991). See, especially Sec. 6.5 and Eq. 6.5.19 in the degenerate electron limit.
[16] E. T. Swartz and R. O. Pohl, Rev. Mod. Phys. **61**, 605 (1989). For a discussion of substrate damage, see pp. 652ff.
[17] D. Kotchetkov, J. Zou, A. A. Balandin, D. I. Florescu, and F. H. Pollak, Appl. Phys. Lett. **79**, 4316 (2001).